Routing and Spectrum Allocation in Elastic Optical Networks: A Tutorial

V. Varalakshmi, S. Leelashyam, M Venkataratnam
Associate Professor, Assistant Professor[2,3]
Department of ECE,
vvaralaxmi.ece@anurag.ac.in, vleelashyam.ece@anurag.ac.in, mvenkataratnam.ece@anurag.ac.in
Anurag Engineering College, Kodada, Telangana

Abstract

We describe an iterative site-based method for estimating the impulse response of optical wireless channels. The method allows for the simultaneous evaluation of channels for many receiver or transmitter locations, thus providing significantly improved calculation times. A simple geometrical model of indoor environments is presented which includes interior features such as partitions, people, and furniture, thus permitting accurate evaluation of shadowing effects. We demonstrate that by considering multiple receiver or transmitter locations, we can improve calculation times by a factor of more than a thousand.
The tool is applied to the problem of developing propagation models for randomly oriented transmit- ters and receivers inside rooms. Our study shows channel gain variations at a fixed transmitter/receiver separation of more than 20 dB. At large separations, receivers with LOS paths to the transmitters receive on average 7 dB more power than those with no LOS. We also show average RMS delay spreads increasing with distance and ranging from 4 ns to 7 ns for non-LOS channels and up to 3 ns for LOS channels. Finally, in furnished rooms we show that accurate estimation of channel parameters requires calculation of at least four-bounce impulse responses.

Index Terms

Optical wireless communications, channel simulation, channel modeling.

INTRODUCTION

High-quality wireless access to information, networks, and computing resources by users of portable computing and communication devices is driving recent activity in indoor optical communication [1], [2], [3], [4]. High-quality access is achieved via links with low delay, high data rates, and reliable performance, and accurate characterization of the channel is essential to understanding the performance limits and design issues for optical wireless links.
We develop a method that calculates impulse responses for wireless optical channels formed by one or more transmitters and receivers placed inside a reflective environment with obstructions. The path loss and multipath dispersion for a particular link configuration will determine many aspects of commu- nication system design as well as optical system design. Electromagnetic waves at optical frequencies exhibit markedly different propagation behavior than those at radio or microwave frequencies. At optical frequencies, most building surfaces are opaque, which generally limits the propagation of light to the transmitter’s room. Furthermore, for most surfaces, the reflected light wave is diffusely reflected (as from a matte surface) rather than specularly reflected (as from a mirrored surface).
These differences, as well as fundamental differences in the transmitting and receiving devices, have led researchers to develop channel and communication concepts for optical wireless systems and channels. In particular, characterization for optical wireless channels has been done by a variety of methods at different levels. Basic system models were developed in [5], [6]. Measurement studies [7], [8], [6] have validated the basic diffuse reflection model and have shown the importance of the orientation of the transmitter and receiver as well as the importance of shadowing. Statistical models of channel characteristics [9] have attempted to make sense of the important factors illustrated in the above measurement studies.
The present work is an extension of [10] to multiple receivers and/or transmitters and to more general receiver effective area and transmitter radiant intensity characterization. Site-specific channel estimation [11], [12], [13], [14], [15] seeks efficient and accurate estimates of impulse response (the path loss and multipath dispersion) based

on the propagation environment, transmitter, and receiver characteristics. The present work is an extension of Barry's method for calculating impulse responses in [11]. His recursive technique is limited to a small number of reflections or bounces k, since its compute time is exponential in
k. As will be shown, the same impulse response can be computed iteratively in time proportional to k2. In
[13], a time-slicing approach is used rather than one based on reflections. In [14], a fast geometric approach is used for calculating impulse responses, but the approach is still limited by computational complexity at higher-reflection orders. In [15], the authors present a mixed ray-tracing–deterministic algorithm for estimating the impulse response. Their approach solves the high-order reflection problem, but introduces estimation error due to the random generation of rays. We present a completely deterministic solution that allows fast, accurate characterization of the channel in complex environments.
In the next section, we describe models for characterizing the properties of transmitters, receivers, and reflecting surfaces within the indoor environment and present an efficient method for impulse response calculation. In Section III, we describe our computer implementation and discuss the computational efficiency of our approach. In Section IV, we present the results of a study of propagation characteristics for a large ensemble of channels in a variety of rooms. Conclusions are presented in Section V.

I. MULTIRECEIVER CHANNEL ESTIMATION

A. Site and Link Model

We model optical wireless channels formed by a transmitter and receiver placed inside a reflective environment, as depicted in Fig. 1(b). The transmitter or source S_j is a laser diode or a light-emitting diode transmitting a signal $X_j(t)$ using intensity modulation (IM). We first consider a collection of receivers, each with a photodiode with responsivity r and using direct detection (DD). These receivers may be either a group of receivers being used as an angle-diversity receiver, as in [16], or they might represent a collection of alternative single receiver locations that are being considered together. We will show that considering all receiver locations and orientations concurrently will bring substantial savings in channel estimation computation time.

1) Channel Model: The signal received by receiver R_i when source S_j is transmitting is $Y_{ij}(t)$, the current from the photodiode:

$$Y_{ij}(t) = rX_j(t) * h_{ij}(t) + N_i(t) \quad (1)$$

where $*$ denotes convolution, $h_{ij}(t)$ is the impulse response of the channel between source S_j and receiver R_i, and $N_i(t)$ is noise at the receiver. This baseband impulse response for IM/DD communication [6] is fixed and completely determined for a given set of source properties S_j, receiver properties R_i, and environment properties E, and hence we will write $h_{ij}(t)$ more specifically as $h_E(t; S_j, R_i)$. Although we consider multiple transmitters and receivers, we restrict our focus in this paper as in (1) to a single transmitter and a single receiver at a time. If multielement transmitters are employed, all active, then the signal received by receiver R_i would be

$$Y_{ij}(t) = \sum^{J} (rX_j(t) \quad h_{ij}(t)) + N_i(t) \quad (2)$$

where the transmitted signals $X_j(t)$ might be carrying the same or different information sequences. A multielement receiver employing combining would receive the signal

$$Y(t) = \sum_{i=1}^{I} \alpha_i Y_{ij}(t - \tau_i). \tag{3}$$

2) Source and Receiver: The source S_j is described by a position vector $\dot{r}_{sj}$, an orientation vector $\hat{n}_{sj}$ and a radiant intensity pattern $T(\varphi)$, where we assume for simplicity that the radiant intensity pattern has axial symmetry about the normal. A typical model for radiant intensity pattern is the Lambertian order n given by

$$T(\varphi) = \frac{n+1}{2\pi}\cos^n(\varphi). \tag{4}$$

The receiver R_i is described by a position vector $\dot{r}_{ri}$, an orientation vector $\hat{n}_{ri}$, an optical collection area A_{ri}, and an effective area at incident angles θ of $A_i(\theta) = A_{ri} g_i(\theta)$. The receiver optical gain function $g_i(\theta)$ is again modeled as axial symmetric. This allows for a very general description of the receiver optical system. A typical model for a bare photodiode is that $g(\theta) = \cos(\theta)$; the cosine dependence models the decline in effective area for light incident on planar detectors at non-normal incidence.

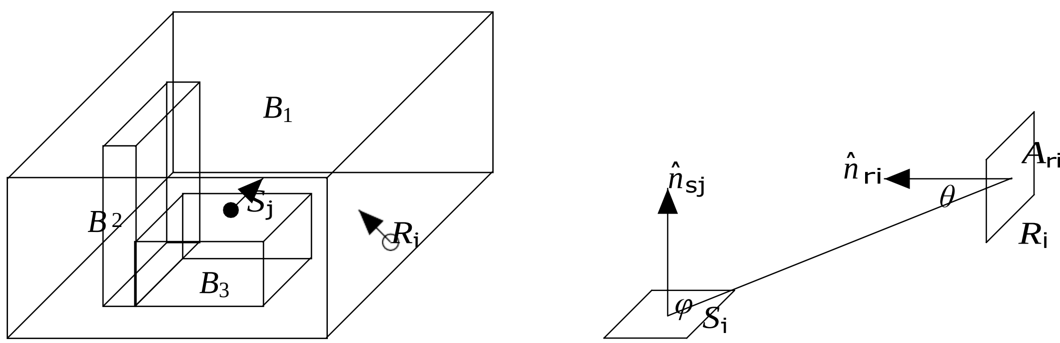

(a) Environment (b) Source and Receiver

Fig. 1

SITE AND LINK MODEL.

3) Environment: The environment E is modeled as a set of N_b rectangular boxes $\{B_1, \ldots, B_{N_b}\}$, as depicted in Fig. 1(a). The first box B_1 represents the "universe" in which all other boxes and all sources and receivers are contained. This can represent a single room, a floor, or even an entire building. Interior objects are described by single boxes or combinations of boxes. This method allows for inclusion of such objects as wall partitions, doorways, desks, chairs, and people. The boxes are further modeled as having six opaque internal faces and six opaque external faces. Only the exterior faces of the internal boxes $B_2, \ldots, B_{N_b}$ are relevant, and only the internal faces of the universe box B_1 are relevant, for a total of $6N_b$ reflecting faces. Each face F_i is modeled as a diffuse reflective surface (Lambertian) of reflectivity ρ_{F_i}. The receivers and transmitters are not included as boxes, so their packaging must be explicitly included if it is significant to the problem at hand.

B. Impulse Response Calculation

Our impulse response calculation follows the basic methodology outlined in [10] with extensions for arbitrary transmitter and receiver gains and multiple transmitters and receivers. The calculation involves decomposition into bounces, discretization into facets, and finally multi-receiver iteration. We then present an equivalent formulation for a multi-transmitter calculation.

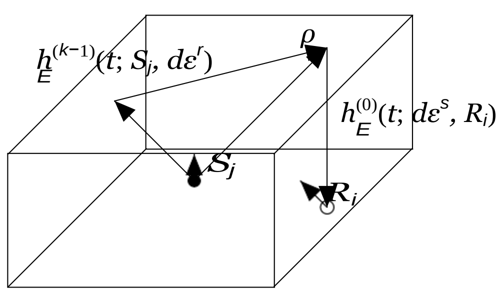

Fig. 2

IMPULSE RESPONSE CALCULATION

1) Decomposition into bounces: All transmitted light arriving at the receiver has undergone a definite number of reflections or bounces. Hence, we can decompose the impulse response $h_E(t; S_j, R_i)$ as

$$h_E(t; S_j, R_i) = \sum^{\infty} h_E^{(k)}(t; S_j, R_i) \quad (5)$$

$k=0$

where $h_E^{(k)}(t; S_j, R_i)$ is the impulse response due to signal light undergoing exactly k bounces during its path from the source S_j to the receiver R_i.

The line of sight impulse response $h_E^{(0)}(t; S_j, R_i)$ is given by

$$h_E^{(0)}(t; S_j, R_i) = V(\dot{r}_{sj}, \dot{r}_{ri}, E)T(\varphi_{ij}) \; A_{ri} g(\theta_{ij})/D_{ij}^2 \; \delta(t - D_{ij}/c) \quad (6)$$

where $D_{ij} = |\dot{r}_{sj} - \dot{r}_{ri}|$ is the distance between the source and the receiver. The visibility function $V(\dot{r}_{sj}, \dot{r}_{ri}, E)$ is 1 when the LOS path between S_j and R_i is unobstructed, and is zero otherwise.

Now, the k-bounce response can be calculated using the $(k-1)$-bounce response using

$$h_E^{(k)}(t; S_j, R_i) = \int_E \rho_{d\varepsilon^r} \cdot h_E^{(k-1)}(t; S_j, d\varepsilon^r) * h_E^{(0)}(t; d\varepsilon^s, R_i) \quad (7)$$

where the integral is over all surfaces in E and ρ is the surface reflectivity function. (see Fig. 2). The quantities $d\varepsilon^s$ and $d\varepsilon^r$ represent a differential surface of area dr^2 that is first acting as a receiver from the source S_j and then as a source to the receiver R_i. The surfaces act as receivers with $g(\theta) = \cos(\theta) \cdot 1\{\theta < \pi/2\}$ and as first-order Lambertian transmitters[1].

[1]The differential component dr^2 does not explicitly appear in (7) since it is included implicitly in the zero-bounce calculation as the area of the sourceTo estimate $h_E(t; S_j, R_i)$ using (5), we consider only the first M bounces so that

II. IMPLEMENTATION AND COMPUTATIONAL EFFICIENCY

We have developed a computer implementation of the models and calculation methods described in Sections II. The program, named IrSimIt, is written in the C programming language and employs a MATLAB interface using the MEX facility. It is available at [17].

computation time primarily depends on (a) the maximum number of bounces considered, M, (b) the number of partitions in the room, N, and (c) the number of receivers considered I. From a derivation

The computation times for a 4x4 m^2 room are shown in Fig. 3. The room contains a single desk modeled as a box, and has a total of $N = 2024$ facets. The calculations were performed on a 1.7 GHz Pentium III processor. As shown in Fig. 3(a), the time to calculate a four-bounce impulse response in this scenario for a single receiver is 23.6 s, whereas we can calculate impulse responses for 10000 different receivers (for the same transmitter) in 213.2 seconds, resulting in a speedup factor of 1.1×10^3.

We can see that for two or more bounces, when up to one hundred receivers are considered the additional complexity to calculate the receiver impulse responses is negligible, and hence the speedup factor is approximately equal to the number of receivers considered. For very large collections of receivers, the compute time will be dominated by the time to calculate the receiver impulse responses $h^k(t; S_j, R_i)$ for each receiver R_i, and not by the time to compute the "surface responses" $h_E^{(k)}(t; S_j, \varepsilon^r_m)$. Thus, the speedup factor eventually is limited to about 10^3 for 2, 3, or 4 bounces for this parameter set. For one-bounce responses, the speedup is much more modest because the most time-consuming operation (calculation of N surface responses from N previous surface responses) is not needed. We are only saved from having to recompute a collection of zero-bounce responses.

III. Propagation Modeling

Using this channel estimation tool, we will investigate propagation characteristics for a large ensemble of transmitter and receiver locations and orientations in a suite of rooms. More than eighty thousand impulse responses were calculated in total, arising from different room sizes, transmitter locations and orientations, and receiver locations and orientations.

Configuration

We create models of empty rooms ranging from small offices to large classrooms and conference rooms. Transmitters are distributed at regular intervals around the room, every two meters on the x- and y-axis, at heights of 1, 2 and 3 meters. As discussed above, IrSimIt allows multiple receivers for each transmitter without significantly increased simulation time. We place ten receivers uniformly distributed over the sphere of radius D_{ij} centered at the transmitter, rejecting any receiver placement that causes a receiver to be outside the room. This will cause certain aspects of the data to not conform to theoretical

expectations, yet gives us a more accurate model of real-world data. The reflectivities of the walls are assumed to be 0.9, the ceiling 0.8 and the floor 0.2. These values are typical of predominantly white rooms; lower values should be considered for furnished indoor environments.

The transmitter radiant intensity pattern is Lambertian. The receiver field-of-view (FOV) is set at $\pi/2$ and the area $A_{ri} = 10^{-4}\text{m}^2$. The orientation angle of the transmitter and receivers is determined by two random variables, the elevation and azimuth. For each transmitter location, ten different angles are

simulated. The azimuth is a uniform random variable between $[0, 2\pi]$, the cosine of the elevation is a uniform random variable between [0, 1]. These are the necessary conditions to have the angles uniformly distributed over a sphere. We assume all transmitters are pointing somewhere into the room to eliminate calculations when a transmitter is facing the wall. The distance (D_{ij}) evaluated between the transmitter and receivers will vary depending on room size.

We initially consider up to two bounces, which provide reasonably accurate impulse responses for bare rooms. In Section IV-D, we will consider the impact of furniture and calculate responses for up to four bounces. Data obtained using two bounces includes three components (1) LOS, (2) first reflection off of all surfaces, and (3) second reflection off all surfaces. Since the rooms are empty, all receiver and transmitter pairs will receive some power. The impulse responses from the simulations are evaluated and two pieces of data are collected, channel gain and root-mean-square delay spread. It has been shown that channel gain and rms delay spread can be sufficient to model diffuse optical wireless channels [9], [16]. Typical impulse responses for a channel with a LOS path and a channel without a LOS path can be seen in Fig. 4.

Channel Gain

Channel gain is defined as the ratio between the received power and the transmitted power. The channel gain in dB is equal to the received power in dBW when 1 W is transmitted. Channel gain is the single most important feature of an optical wireless channel, as it determines the achievable signal-to-noise ratio for fixed transmitter powers and is important regardless of the data rate or modulation scheme employed [1].

Fig. 5 shows typical channel gain distributions of the data collected from IrSimIt. Although only data for a 4x4 m^2 room is shown, all rooms measured experienced similar trends. When analyzing the histograms, we notice that two distinct curves exist. We hypothesize that having a LOS component in

the channel may be causing this effect. Hence in Fig. 5 the channels containing a LOS component are highlighted. As D_{ij} increases, the channel gain distribution of the LOS channels merges with that of thechannels containing no LOS path. As shown in (6), the LOS path $h^{(0)}()$ is inversely proportional to D^2,

E ij

causing the LOS component to become less prominent at large values of D_{ij}. The distributions of the no LOS channels fall in a similar channel gain range for all D_{ij}.

Fig. 6 shows the mean channel gain of various rooms versus D_{ij}. As expected from (6) the LOS channel gain falls off proportional to D^2 . The LOS channels exhibit much stronger channel gains than the non-LOS channels, particularly for small distances. The average received power gap between LOSand non-LOS channels for distances greater than 2 m is about 7 dB.

The mean curve from channels with no LOS component exhibits interesting behavior. One would expect that room size would have more of an effect on channels with no LOS component. A room with a smaller area should experience stronger channels because the signals do not have as far to travel. Looking at the graph this seems to be mostly true. However the dependency does not seem to be strictly on area, but on shortest wall. For example, the 4x4 and 4x8 rooms remain close to each other, as do the 8x8 and

Multipath Dispersion

It is important not only to look at channel gain but also the rms delay spread of the signal. The delay spread will be increasingly important for higher data rates [1]. For example, when $S = 0.2/R$, where R is the data rate, the power penalty for on-off keying modulation is about 2 dB for typical channels.

Thus, delay spreads of 4 ns cause power penalties of 2 dB at a data rate of 50 Mb/s. Schemes such as PPM that employ narrow pulses are even more susceptible to delay spread effects.

$$\mu = \left(\sum t h^2(t) \right) / \left(\sum h^2(t) \right). \quad (19)$$

Fig. 7 shows typical rms delay spread distributions of the data collected from IrSimIt. The room size and values of D_{ij} correspond to Fig. 5. Notice here that a large majority of the small delay spread values have a LOS channel. At D_{ij} = 0.1 m the delay spread (S) is 0.03 ns on average for all different room sizes. The delay spread is especially low here and at D_{ij} = 0.2 m because the power received from the LOS component is so strong that additional power from the first and second bounce are virtually null. As distance increases the initial power received from the LOS path falls off, making any additional multi-path components more effective.

The channels with no LOS path experience much higher delay spread values. Most values fall in the range between 1-7 ns, and the mean is approximately 4-5 ns more than the LOS channels. The histograms of no LOS channels are relatively uniform between 2-5 ns. These are the most common values and represent 60% of the no LOS samples. The values preceding and following this range resemble an exponential distribution.

Fig. 8 shows a general increase in the mean delay spread for both LOS and no LOS channels as delay spread increases. For LOS channels, the LOS component will dominate the curve and there is a direct correlation between distance and LOS transmission time. For all room sizes at close distance there is no apparent trend in the no LOS delay spread data. As D_{ij} increases past 1.0 m the larger rooms begin to show a definite increase. The smaller 4x4 m^2 and 4x8 m^2 rooms shows a linear trend. Because of the small room sizes, the distance between the transmitter and receiver has less impact on the no LOS channel.

Rooms with Objects

Now we shall discuss some data from a simulation of a 4x4 m^2 office with furniture. The office is shown in Fig. 9 with a bookcase, file cabinet, table (legs are not shown because they are negligible), desk and partition.

CONCLUSIONS

Multipath impulse response estimation for optical wireless IM/DD channels can be performed ac- curately and efficiently using the described iterative site-based model and computer implementation. Complex reflection environments can be modeled, which allows for inclusion of shadowing and related effects. The method allows for complex receiver gain and transmitter intensity and can account for multiple reflections of any order. In particular, it makes practical the calculation of four-bounce (or more) impulse responses.

We demonstrated a method for improving calculation times when multiple transmitter or receiver locations are to be evaluated. Calculation times can be reduced by a factor of more than 10^3 when many receivers are considered. The speedup factor is approximately equal to the number of receivers considered for up to one hundred receivers.

Our study shows channel gain variations of more than 20 dB at a fixed transmitter/receiver separation. At large separations, receivers with LOS paths to the transmitters receive on average 7 dB more power than those with no LOS path. The channel gain variation with distance is more substantial for LOS channels than for non-LOS channels. We also show average RMS delay spreads increasing with distance and ranging from 4 ns to 7 ns for non-LOS channels and up to 3 ns for LOS channels. In furnished rooms, including up to four bounces in the impulse response calculation provides better channel estimates, increasing the estimates of both channel gain and delay spread.

References

J. M. Kahn and J. R. Barry, "Wireless infrared communications," *Proceedings of the IEEE*, vol. 85, no. 2, pp. 265–98, Feb. 1997.

D. Heatley, D. Wisely, I. Neild, and P. Cochrane, "Optical wireless: The story so far," *IEEE Communications Magazine*, pp. 72–82, Dec. 1998.

Infrared Data Association standards can be obtained at the organization's home page on the World Wide Web: http://www.irda.org.

IEEE 802.11 Standard Working Group, *Wireless LAN Medium Access Control (MAC) and Physical Layer (PHY) Specifications*. IEEE, 1997.

F. R. Gfeller and U. H. Bapst, "Wireless in-house data communication via diffuse infrared radiation," *Proceedings of the IEEE*, vol. 67, no. 11, pp. 1474–1486, Nov. 1979.

J. M. Kahn, W. J. Krause, and J. B. Carruthers, "Experimental characterization of non-directed indoor infrared channels,"
IEEE Transactions on Communications, vol. 43, no. 2-3-4, pp. 1613–1623, February-March-April 1995.

H. Hashemi, G. Yun, M. Kavehrad, F. Behbahani, and P. Galko, "Frequency response measurements of the wireless indoor channel at infrared optics," in *International Zurich Seminar on Digital Communications*, Mar. 1994.

——, "Indoor propagation measurements at infrared frequencies for wireless local area networks applications," *IEEE Transactions on Vehicular Technology*, vol. 43, no. 3, pp. 562–576, Aug. 1994.

J. B. Carruthers and J. M. Kahn, "Modeling of nondirected wireless infrared channels," *IEEE Transactions on Communi- cations*, no. 10, pp. 1260–1268, Oct. 1997.

J. B. Carruthers and P. Kannan, "Iterative site-based modeling for wireless infrared channels," *IEEE Transactions on Antennas and Propagation*, vol. 50, pp. 759–765, May 2002.

J. R. Barry, J. M. Kahn, W. J. Krause, E. A. Lee, and D. G. Messerschmitt, "Simulation of multipath impulse response for indoor wireless optical channels," *IEEE Journal on Selected Areas in Communications*, vol. 11, no. 3, pp. 367–379, Apr. 1993.

M. Abtahi and H. Hashemi, "Simulation of indoor propagation channel at infrared frequencies in furnished office

environments,” in *PIMRC*, 1995, pp. 306–310.
F. Lopez-Hermandez and M. Betancor, “DUSTIN: algorithm for calculation of impulse response on IR wireless indoor channels,” *Electronics Letters*, vol. 33, pp. 1804–1806, Oct. 1997.
D. Mavrakis and S. R. Saunders, “A novel modelling approach for wireless infrared links,” in *Proceedings of 3rd International Symposium on Wireless Personal Multimedia Communications (WPCS’00)*, 2000, pp. 609–614.
F. J. Lopez-Hernandez, R. Perez-Jimenez, and A. Santamaria, “Ray-tracing algorithms for fast calculation of the channel impulse response on diffuse IR wireless indoor channels,” *Optical Engineering*, vol. 39, pp. 2775–2780, 2000.
J. B. Carruthers and J. M. Kahn, “Angle diversity for nondirected wireless infrared communication,” *IEEE Transactions on Communications*, June 2000.
J. B. Carruthers and P. Kannan, “IrSimIt,” http://iss.bu.edu/bwc/irsimit.
P. Kannan, “Iterative site-based modeling for wireless infrared channels: an analysis and implementation,” Master’s thesis, Boston University, Dept. of Electrical and Computer Engineering, 2001.